Analytica Chimica Acta 1187 (2021) 339155

Contents lists available at ScienceDirect

Analytica Chimica Acta

journal homepage: www.elsevier.com/locate/aca

An efficient SERS platform for the ultrasensitive detection of *Staphylococcus aureus* and *Listeria monocytogenes* via wheat germ agglutinin-modified magnetic SERS substrate and streptavidin/aptamer co-functionalized SERS tags

Siyun Cheng [a, b, 1], Zhijie Tu [a, b, 1], Shuai Zheng [b, d], Xiaodan Cheng [b, d], Han Han [b], Chongwen Wang [a, b, d, *], Rui Xiao [b, **], Bing Gu [a, c, ***]

[a] Medical Technology School of Xuzhou Medical University, Xuzhou, 221004, PR China
[b] Beijing Institute of Radiation Medicine, Beijing, 100850, PR China
[c] Laboratory Medicine, Guangdong Provincial People's Hospital, Guangdong Academy of Medical Sciences, Guangzhou, 510000, PR China
[d] College of Life Sciences, Anhui Agricultural University, Hefei, 230036, PR China

HIGHLIGHTS

- A rapid and ultrasensitive SERS platform for *S. aureus* and *L. mono* detection was reported.
- WGA modified-Fe_3O_4@Au MNP was proposed for broad-spectrum capture of multiple bacteria.
- The SA/aptamer co-functionalized SERS tags exhibited higher affinity and stability.
- The LODs for *S. aureus* and *L. mono* were 3 and 5 cells/mL, respectively.

GRAPHICAL ABSTRACT

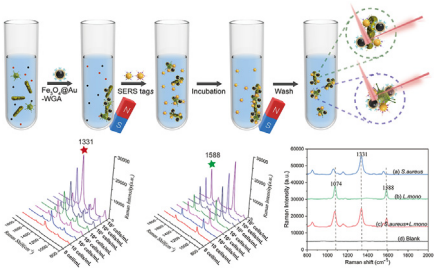

ARTICLE INFO

Article history:
Received 31 July 2021
Accepted 4 October 2021
Available online 7 October 2021

Keywords:
SERS
WGA
Pathogenic bacteria
Multiplex detection
Dual-recognition

ABSTRACT

A novel surface-enhanced Raman scattering (SERS)-based analytical technique was proposed to simultaneously detect two highly pathogenic bacteria, namely, *Staphylococcus aureus* (*S. aureus*) and *Listeria monocytogenes* (*L. mono*) by using a dual-recognition pattern with wheat germ agglutinin (WGA) and nucleic acid aptamers. WGA was modified onto Fe_3O_4@Au magnetic nanoparticles (MNPs) for the efficient capture of *S. aureus* and *L. mono* in complex samples (orange juice, extracts of lettuce, and human urine) within 15 min. The streptavidin (SA)/aptamers co-functionalized SERS tags were fabricated by covalent attaching two different Raman reporters and SA molecules onto 45 nm Au NPs and then conjugated with two biotin-aptamers that specifically bind to their target bacteria with high affinity and stability. The combined use of high-sensitive SERS tags, WGA-mediated magnetic enrichment, and SA-mediated aptamer conjugation remarkably improved the assay sensitivity. Under optimized conditions, the developed SERS biosensor can simultaneously detect the two target bacteria with high detection sensitivity (<6 cells/mL), favorable linear relation (10-10^7 cells/mL), and high accuracy

* Corresponding author. Medical Technology School of Xuzhou Medical University, Xuzhou, 221004, PR China.
** Corresponding author.
*** Corresponding author. Medical Technology School of Xuzhou Medical University, Xuzhou, 221004, PR China.
E-mail addresses: wangchongwen1987@126.com (C. Wang), ruixiao203@sina.com (R. Xiao), gb20031129@163.com (B. Gu).
[1] The authors Siyun Cheng and Zhijie Tu contributed equally to this work.

https://doi.org/10.1016/j.aca.2021.339155

(recovery rate <7.03%). Therefore, the proposed SERS platform is rapid, sensitive, easy to use, and thus show potential as a tool for the timely identification of pathogenic bacteria in real samples.

1. Introduction

Pathogenic bacteria such as *Staphylococcus aureus* (*S. aureus*), *Listeria monocytogenes* (*L. mono*), *Escherichia coli* O157:H7 (*E. coli* O157:H7), and *Salmonella typhimurium* (*S. typhi*), are always a major concern to food safety and public health and cause 550 million infections worldwide and nearly 5.2 million deaths a year [1,2]. Accurate and sensitive identification of etiologic agent in food products and clinical samples is essential to control bacterial infections and ensure food safety and health at the source. The currently approved approaches for accurate pathogen detection in testing organization mainly include culture-based methods [3], polymerase chain reaction (PCR) [4], mass spectrometry [5], and nucleotide sequencing method [6]. All these techniques are limited by some disadvantages, such as requiring long testing time (3–72 h), laborious sample pretreatment, expensive instruments, and high cost, which greatly limit their application in rapid analysis [7]. A rapid and sensitive platform for the simultaneous identification of multiple pathogens in complex samples is urgently needed.

In recent years, many nanomaterial-based biosensors, including electrochemical biosensor [8], surface plasmon resonance (SPR) [9], fluorescence signal-based method [10], and surface enhanced Raman scattering (SERS) [11], have been proposed by utilizing sensitive chemical or optical signal to achieve the rapid and accurate identification of low concentration pathogen. Among them, SERS label technology has attracted great attention for the ultrasensitive and quantitative analysis of biochemical molecules because of its ability to provide strong (single-molecule level), stable (no photobleaching), and quantifiable optical signals by using specific Raman reporters modified Au/Ag nanoparticles (NPs) [12–14]. When magnetic nanomaterials (MNMs) are further introduced into the biosensors, the target bacteria could be efficient captured and enriched by biorecognition molecule-modified MNMs from the complex solution, thus avoiding sample pretreatment, shortening detection time, and improving the sensitivity [15–17]. Zheng's group used antibody-modified magnetic nanoparticles (MNPs) as magnetic separation tool and aptamer-conjugated gold nanoparticles (AuNPs) as SERS-label tags to simultaneously detect *E. coli* O157:H7 and *S. typhi* with low limit of detection (LOD) (10 cfu/mL) [18]. Our group previously proposed a method of combining vancomycin-labeled magnetic gold nanoparticles and aptamer-modified SERS tags to directly detect *S. aureus* and *E. coli* in real clinical samples [19].

Notably, the performance of these biosensors for target pathogen highly depends on the recognition and binding ability of their biorecognition molecules. Only several kinds of biorecognition agents, which mainly include antibodies, aptamers, antibiotic (e.g., vancomycin), antimicrobial peptides, and phages, could be used to build MNMs-based biosensors [20–24]. Most of these biorecognition molecules have one or more disadvantages to achieve the universal detection of multiple bacteria. For example, antibodies are expensive, difficult to prepare, and subject to poor reproducibility [25]. Aptamers with high affinity to bacteria are quite challenging to screen [26]. In addition, the binding of the aptamer with target bacteria usually requires high-salt ions, which may affect the stability of colloidal SERS tags. Antibiotics and peptides generally lack high affinity and specificity to a large proportion of pathogens, and phages are hard to be modified onto the nanomaterial surface to realize effective functionalization. The deficiencies of the currently used bacterial biorecognition molecules severely limit the development of broad-spectrum and high-performance biosensor [27]. Thus, exploiting new recognition patterns of SERS label method for bacteria with high affinity and universality is urgently needed.

As one of the most widely characterized lectins, wheat germ agglutinin from *Triticum vulgaris* (wheat) (WGA) is a broad-spectrum recognition molecule for pathogen because it can bind specifically and tightly to N-acetyl-D-glucosamine and its derivatives on the bacterial surface via multiple forces (e.g., hydrophobic interactions, hydrogen bonding and electrostatic interactions) [28–30]. This lectin has strong affinity to a broad spectrum of pathogens including gram-positive (e.g., *S. aureus*) [31] and gram-negative bacteria (e.g., *E. coli* O157:H7) [32,33]. Given its easy modification, low cost and high stability, WGA is a good candidate as high-performance recognition reagent to build biosensor for the simultaneous detection of multiple bacteria [34].

In this study, a magnetic-assisted SERS platform was proposed for the ultrasensitive detection of two highly pathogenic bacteria, namely, *S. aureus* and *L. mono*, by using WGA and aptamers as dual-recognition reagents. *S. aureus* and *L. mono* are two of the most influential gram-positive foodborne pathogens that can contaminate various foods and survive in vacuum packaging environment, thereby easily causing severe food poisoning with high mortality rate [35,36]. The WGA-modified Fe_3O_4@Au MNPs were used as efficient bacteria enrichment tools with high capture efficiencies (>90%) and short capture time (<15 min) for the two target bacteria. Streptavidin (SA)/aptamer co-functionalized SERS tags were fabricated to greatly increase the amounts of aptamers loaded onto the AuNP surface and improve the stability of SERS tags in high-salt solutions. The detection sensitivity of the proposed SERS-label platform was substantially improved by the combination of high-sensitive SERS signals of SERS tags, WGA-mediated magnetic enrichment, and SA-mediated four-fold increase in aptamer conjugation. Under optimal conditions, *S. aureus* and *L. mono* were quantitatively detected within $10–10^7$ cells/mL with LODs of 3 and 5 cells/mL, respectively. Sandwich SERS-based assays were also successfully applied for the detection of *S. aureus* and *L. mono* in real food samples (orange juice and extracts of lettuce) and human urine. To the authors' best knowledge, this study is the first application of WGA and SERS tags to detect multiple bacterial pathogens. The proposed dual-recognition SERS platform offers new perspectives for the universal and efficient detection of bacteria in food safety and health inspections.

2. Experimental

2.1. Materials and apparatus

WGA, bovine serum albumin (BSA), polyvinylpyrrolidone (PVP, 40 kDa), 5,5′-dithiobis-(2-nitrobenzoic acid) (DTNB), N-(3-dimethylaminopropyl)-N′-ethylcarbodiimide (EDC), 4-mercaptobenzoic acid (4-MBA), N-hydroxysuccinimide (NHS), 2-(N-morpholino) ethanesulfonic acid (MES), 11-mercaptoundecanoic

acid (MUA), polyethyleneimine (PEI), Tween-20, and SA were purchased from Sigma–Aldrich (USA). Chlorauric acid tetrahydrate ($HAuCl_4 \cdot 4H_2O$), phosphate-buffered saline (PBS, pH 7.4), trisodium citrate (TSC), hydroxylamine hydrochloride, and ethanolamine were obtained from Sinopharm Chemical Reagent Co. (Shanghai). *S. aureus, L. mono, Staphylococcus epidermidis* (*S. epidermidis*), *S. typhi, Acinetobacter baumannii* (*A. baumannii*), *E. coli,* and *Pseudomonas aeruginosa* (*P. aeruginosa*) were provided by Xiao's group [37]. The target bacteria (*S. aureus* and *L. mono*) were cultivated in Trypticase soy broth medium and then verified by PCR (Fig. S1). The primers sequences and their target gene used in this study are provided in Table S1. The exact concentration of bacterial samples was determined by plate counting. The aptamer of *S. aureus* and *L. mono* were synthesized by Sangon Biotech (Shanghai, China), and their sequences are listed in Table S2.

The zeta potential and dynamic light scattering (DLS) data were recorded by using Malvern Nano-ZS90 Zetasizer. The UV–vis spectra of nanomaterials were detected by a Shimadzu 2600 spectrometer. The structure and morphology of Fe_3O_4@Au-WGA, SERS tags and nanomaterials/bacteria complexes were characterized by a Hitachi H-7650 microscope operating at 80 kV. All Raman spectra were collected on a B&W Tek, i-Raman Plus BWS465–785H spectrometer. The acquisition time for sample Raman detection was typically 10 s. A 785 nm laser with 10 mW power was used for sample excitation. For SERS detection, each sample was measured at 10 random spots on Fe_3O_4@Au/bacteria complexes fixed on a Si chip. Each spectrum used for analysis was the average of the 10 SERS spectra.

2.2. Preparation of Fe_3O_4@Au-WGA MNPs

The synthesis process of Fe_3O_4@Au-WGA MNPs is shown in Scheme 1A. First, monodispersed Fe_3O_4@Au core-shell MNPs were prepared according to our previous methods [38,39]. Second, surface-carboxylated Fe_3O_4@Au MNPs were obtained by sonicating 1 mg of Fe_3O_4@Au MNPs in 1 mL of MUA ethanol solution (30 μM) for 1 h. Fe_3O_4@Au MNPs-MUA were then magnetically separated and resuspended in 500 μL of MES buffer (0.1 M, pH 5.5). Freshly prepared EDC (5 μL, 100 mM) and NHS (10 μL, 100 mM) were sequentially added into the above solution to activate the carboxyl groups on the Au shell [40]. After the reaction for 15 min, 5 μL of WGA (10 mg/mL) was then added to link the active Fe_3O_4@Au through amino-carboxyl condensation. The mixture was shaken at 37 °C for 2 h. Finally, the unreacted carboxyl sites of Fe_3O_4@Au-WGA MNPs were blocked with 100 μL of BSA (10%) for an additional 1 h at 37 °C. The final products were magnetically separated, washed twice with 0.05% PBST, and then re-suspended in 500 μL PBST buffer at 4 °C for further use.

2.3. Preparation of SA/aptamer co-functionalized SERS tags

The synthesis process of AuNPs modified by SA is illustrated in Scheme 1B. Au NPs with 45 nm particle size were synthesized as previously described [16]. In brief, 1 mL of 1% $HAuCl_4$ (w/v) and 1 mL of 1% TSC was mixed and boiled under stirring (100 °C) for 15 min and then cooled to room temperature. Raman reporters DTNB (100 μL, 10^{-2} M) or MBA (40 μL, 10^{-2} M) were then added to 100 mL of Au NPs and stirred vigorously at room temperature for 4 h. The centrifugation process (5600 rpm, 7 min) was conducted to remove the redundant Raman molecules and then resuspend in 1 mL of MES buffer (10 mM, pH 5.5). Finally, the biotin-modified aptamers and Au NPs were coupled through SA-biotin reaction to prepare SERS nanotags for bacterial specific recognition. In brief, 5 μL of EDC (10 mM) and 10 μL of NHS (10 mM) were added to 1 mL of the as-prepared DTNB/MBA-modified Au NPs and then vigorously shaken for 15 min. After being centrifuged at 5400 rpm for 6 min, the precipitate was resuspended in 500 μL of PB buffer (2 mM, pH 7.4) and then added with 2 μg of SA to link AuNPs through amide condensation. After incubation for 2 h, the formed AuNP/DTNB/SA or AuNP/MBA/SA was separated through

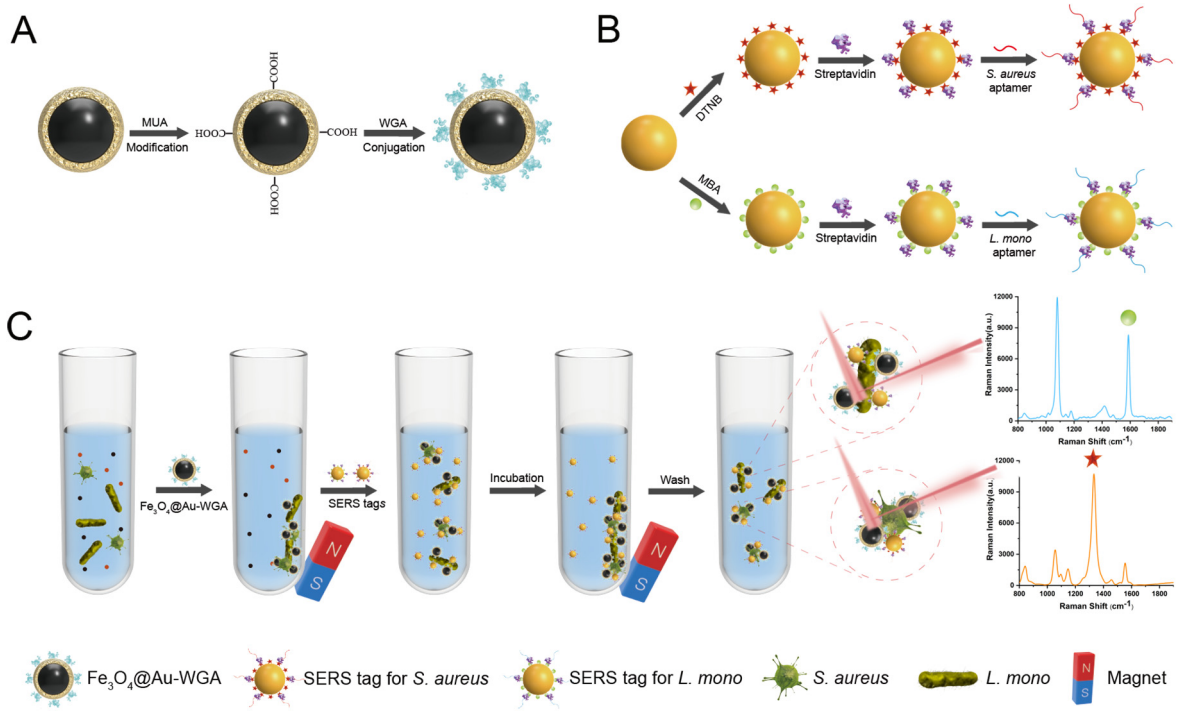

Scheme 1. Illustration of (A) the fabrication of WGA-conjugated Fe_3O_4@Au MNPs, (B) the synthesis of two different SA/aptamer co-functionalized SERS tags for *S. aureus* and *L. mono*, and (C) the principle of the proposed platform for the simultaneous detection of two target pathogens.

centrifugation, redispersed in 1 mL PBS (10 mM, pH7.4), added with 20 μL of biotin-modified aptamer (10 mM), and shaken for another 2 h. Afterward, 100 μL of BSA (1%, w/v) solution was used to deactivate the unreacted the SA-conjugated for 1 h. The final solution was centrifuged at 5600 rpm for 7 min to purify SERS tags and resuspended in 500 μL of PB (2 mM, pH 7.4).

2.4. Preparation of bacterial sample

Bacterial concentrations were verified via classical plate count method. All standard bacterial strains including (*S. aureus*, *L. mono,* and six non-target strains) were incubated in Trypticase soy broth or Luria–Bertani broth medium at 37 °C for 6 h. Then, 100 μL of bacterial culture solution was diluted 10^5 and 10^6 times with LB medium and cultured at 37 °C overnight. Afterward, the number of bacteria was counted. The remaining bacteria were harvested through centrifugation at 4500 rpm for 4 min, washed twice with PBS, and then adjusted to concentration of 10^8 cells/mL.

2.5. Capture efficiency verification

Capture efficiency experiment was conducted as follows. First, the bacteria suspensions were serially diluted to 10^4 cells/mL and then mixed with 10 μL of Fe_3O_4@Au-WGA MNPs (10 mg/mL). The mixture was gently shaken for 15 min with an oscillator. After the Fe_3O_4@Au-WGA-bacteria were magnetically separated, the supernatant from each group (100 μL) was spread on blood plates at 37 °C overnight. Capture efficiency was determined by calculating the difference between the number of the remaining bacteria in the supernatant of control group and captured groups.

2.6. Detection of bacteria by SERS strategy

In a typical experiment, various bacterial concentrations were incubated with 5 μL of Fe_3O_4@Au-WGA MNPs (10 mg/mL) in PBS buffer (pH 7.4, containing 10 mM NaCl, 1 mM Ca^{2+} and 1 mM Mg^{2+}). The formed Fe_3O_4@Au-WGA/bacteria complexes were rapidly separated and washed once with PBST. Afterward, 160 μL of PB buffer (2 mM, pH 7.4, containing 10 mM Mg^{2+}) and 60 μL of SERS tags were added and the mixture was shaken for 45 min to allow the binding of aptamer-conjugated SERS tags with target bacteria. Finally, the formed sandwich complexes were magnetically collected, washed once with water containing 0.05% Tween 20, and transferred onto a Si chip for SERS detection.

3. Results and discussion

3.1. Principle of the SERS biosensor

A high-performance SERS-label biosensor for bacteria sensitive detection was construct by using a dual-recognition strategy based on the efficient and broad-spectrum capture ability of WGA-modified Fe_3O_4@Au MNPs and specific binding ability of SA/aptamer co-functionalized SERS tags (Scheme 1). Relative to previous SERS label-based bacteria detection methods, the major innovations of the proposed strategy could be explained in three aspects. First, monodispersed magnetic nanosphere (~200 nm) with roughness Au shell was employed as a multifunction platform that provides strong magnetic enrichment capacity and excellent SERS property to further enhance the characteristic signal of SERS tags. Second, WGA molecules were modified onto the Fe_3O_4@Au carrier to offer broad-spectrum recognition ability and high affinity for *S. aureus* and *L. mono* in a complex environment. Third, SA was introduced into SERS tags to improve the stability of AuNPs and the coupling efficiency of aptamer.

Scheme 1C illustrates the detection process of the proposed dual-recognition SERS immunoassay platform for the two target bacteria. The Fe_3O_4@Au-WGA MNPs were added into sample solution which contain one or more species of bacteria and incubated for 15 min. During this process, Fe_3O_4@Au-WGA anchored onto the bacterial surface via strong hydrogen bonding and hydrophobic interactions between WGA molecules and the bacterial cell wall. The Fe_3O_4@Au-WGA-bacteria complexes were then magnetically separated and incubated with specific aptamer-modified SERS tags for 45 min to form Fe_3O_4@Au-bacteria-SERS tags with sandwich configurations. The obtained sandwich complexes were rinsed once with PBST solution to remove excess SERS tags via magnetic separation, and their characteristic Raman signals (DTNB for *S. aureus* and MBA for *L. mono*) were measured by a Raman instrument. The generated signal intensity of sandwich complexes was proportional to the bacterial concentration in the samples. This result provides the foundation for quantitative analysis. On the basis of the efficient bacterial enrichment of Fe_3O_4-WGA@Au MNPs and the multi-stage amplification effect between novel SA-Au NPs and biotin-aptamers, the highly sensitive simultaneous quantification of target bacteria could be realized.

3.2. Characterization of Fe_3O_4@Au-WGA MNPs and SA/aptamer co-functionalized SERS tags

Scheme 1A and B shows the synthesis process of Fe_3O_4@Au-WGA MNPs and SERS tags, respectively. As the core of multifunctional platform, the monodispersed Fe_3O_4@Au MNPs were fabricated using our previous PEI-mediated seed growth strategy [13,38]. MUA molecules were then directly coated onto the Au surface of Fe_3O_4@Au MNPs via Au–S bond, which act as linkers and provide terminal carboxyl groups for lectin conjugation [41]. Fig. 1A and B displays the typical TEM images of Fe_3O_4 and Fe_3O_4@Au MNPs, respectively. With the Au shell formed outside the 200 nm Fe_3O_4 core, the diameter of Fe_3O_4@Au MNPs was increased to 250 nm. EDS elemental mapping was used to confirm the structural composition of the prepared nanocomposites. Fig. 1C shows that dense Au elements (green) were homogeneously distributed on the surface of Fe (red) core, indicating the core-shell structure of Fe_3O_4@Au MNPs. WGA was conjugated onto the surface of Fe_3O_4@Au-MUA via carbodiimide chemistry. Fig. S2A shows that the zeta potential of Fe_3O_4@Au-MUA increased from −19.7 mV to eventually −11.2 mV when the WGA was modified, thus implying the successful preparation of Fe_3O_4@Au-WGA.

The ~45 nm citrate-capped AuNPs were used as the basis for designing SERS tags due to their high signal enhancement and good versatility [42]. Two common Raman reporters DTNB and MBA, which contain sulfhydryl and carboxyl groups, were separately modified onto the AuNP surface through the Au–S bond [43]. The characteristic SERS spectra of AuNP/DTNB and AuNP/MBA are displayed in Fig. S3, and the major characteristic bands of DTNB (1059, 1331, and 1558 cm^{-1}) and MBA (1077 and 1588 cm^{-1}) were observed. Two nonintersecting Raman peaks of DTNB (1331 cm^{-1}) and MBA (1588 cm^{-1}) were selected for the quantitative analysis of *S. aureus* and *L. mono* in one test, respectively. As a dual-functional linker, SA was directly modified onto the surface carboxyl groups of AuNP/DTNB and AuNP/MBA to enhance the coupling efficiency of aptamers via biotin-SA interaction and improve the colloidal stability of SERS tags in complex sample. The formation of aptamer-SA-SERS tags was characterized by TEM observation, DLS, and zeta potential measurement. The TEM image from Fig. 1D displays that the fabricated SERS tags were monodispersed with a diameter of ~50 nm. DLS results revealed that the mean diameter of AuNPs increased from 46 nm to 52 nm after SA and aptamer modification (Fig. 1E). The zeta potential values of SERS tags substantially

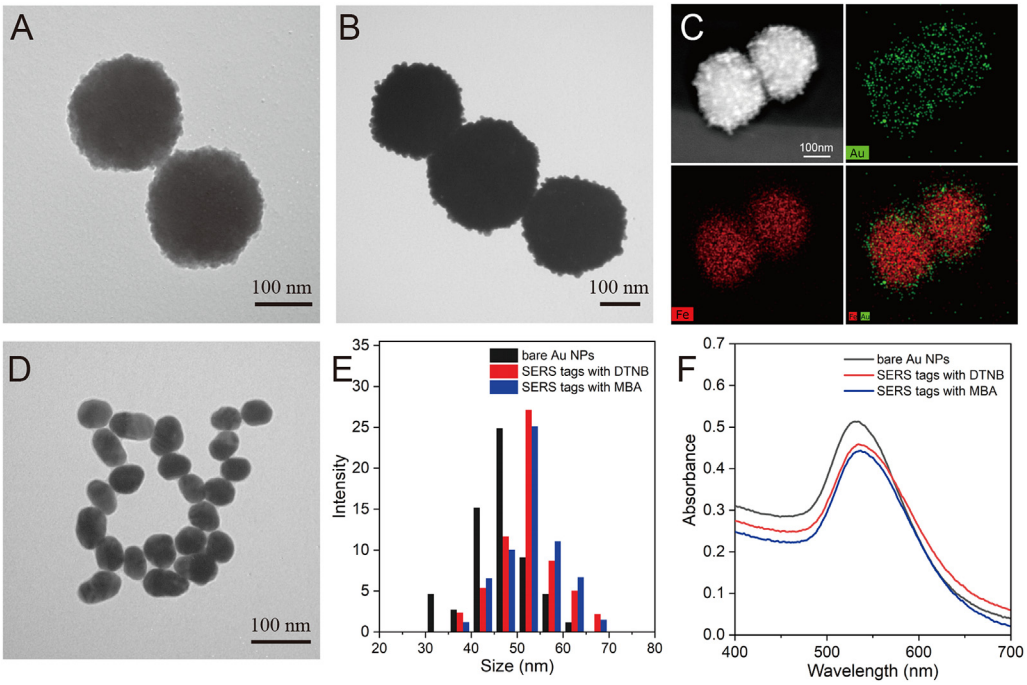

Fig. 1. Characterization of the fabricated nanomaterials. (A–B) TEM images of Fe_3O_4 MNPs (A) and Fe_3O_4@Au MNPs (B). (C) EDS mapping results of Fe_3O_4@Au MNPs. (D) TEM image of AuNP-SA-aptamer tags. (E) DLS distributions and (F) UV–vis absorption spectra of bare AuNPs, and AuNP-SA-aptamer tags with DTNB or MBA loading.

declined after aptamer conjugation and remained stable after incubation with 200 nM aptamer. This finding indicated that the aptamers coupled onto SERS tags reached saturation (Fig. S2B). In addition, the UV–vis spectra showed that the surface plasmon band of SERS tags was slightly red-shifted from 531 nm to 534 nm after SA and aptamer conjugation, thus confirming that the SERS tags did not agglomerate during synthesis (Fig. 1F).

3.3. Verification of the bacterial capture efficiency of Fe_3O_4@Au-WGA MNPs

As a broad-spectrum bacterial recognition agent, WGA has high affinity with N-acetylglucosamine and its derivatives on the surface of Gram-positive and Gram-negative bacteria. In this work, WGA was modified onto surface of Fe_3O_4@Au MNPs to construct an efficient and general tool for bacteria broad-spectrum capture. The capture efficiency of Fe_3O_4@Au-WGA for common pathogenic bacteria should be first investigated. Eight species of Gram-positive and Gram-negative pathogens, namely, *S. epidermidis*, *P. aeruginosa*, *S. aureus*, *L. mono*, *E. coli*, *A. baumannii*, *S. sonnei*, and *S. typhi* were selected to prepare standard bacterial samples (~10^3 cells/mL) to test the capture ability of Fe_3O_4@Au-WGA via conventional culture-based method. As shown in Fig. S4, Fe_3O_4@Au-WGA achieved the effective separation of these bacteria from PBS solution with efficiency of 41%–94%. The differences in capture efficiency may be caused by the varying components (mainly saccharide types) of the bacteria cell. The capture efficiency of Fe_3O_4@Au-WGA for *S. epidermidis, P. aeruginosa, E. coli, S. aureus,* and *L. mono* was >70%, which provided the basis for building the universal capture tool for these bacteria.

The competence of Fe_3O_4@Au-WGA MNPs to capture *S. aureus* and *L. mono* was further evaluated by incubating it with bacterial solution at different concentrations (10 cells/mL–10^4 cells/mL) in PBS buffer for various periods (5–25 min). After the magnetic separation of Fe_3O_4@Au-WGA-bacteria complex, the remaining bacteria in the supernatant were counted by using plate culture (Fig. 2A). The enumeration results in Fig. 2B show that the Fe_3O_4@Au-WGA MNPs exhibited high bacterial-capture efficiency (73.2%–94.2%) for both target bacteria at low concentrations (10^4–10 cells/mL). This finding indicated the feasibility of small number bacterial detection in solution. Controlled trials showed that the unmodified Fe_3O_4@Au MNPs cannot capture bacteria (Fig. S5). In addition, the TEM images in Fig. 2D and E confirmed that the WGA-modified Fe_3O_4@Au MNPs can effectively capture *S. aureus* and *L. mono* from sample solution and generate stable complexes. Fig. 2C displays the relationship between the bacterial capture rates of Fe_3O_4@Au-WGA and reaction time. A 15 min of incubation was sufficient for *S. aureus* and *L. mono* capture. pH 4.0–10.0 had no effect on the capture of *S. aureus* and *L. mono*, thus implying the stable binding ability of Fe_3O_4@Au-WGA in a wide pH range (Fig. S6). These results revealed the excellent capability of Fe_3O_4@Au MNPs to recognize and capture target bacteria and its potential to serve as the ideal magnetic enrichment platform for SERS-label biosensor construction.

3.4. Optimization of the SA/aptamer co-functionalized SERS tags

A typical SERS tags for bacteria detection must have the following three parts: (i) a noble metal (Au or Ag) nanomaterial as the SERS substrate, (ii) loaded Raman dye molecule to provide feature signal, and (iii) surface-modified detection molecules (e.g., antibody, aptamer, and antibiotic) to recognize target bacteria. Direct conjugation has been used to prepare aptamer-modified SERS tags via the amide reaction. Although this method could conveniently conjugate the amino aptamers to SERS tags, the limited amount of aptamers loaded onto the surface of these nanotags may affect the binding efficiency between SERS tags and bacteria. Herein, a layer of SA was incorporated onto the surface of AuNP-DTNB and AuNP-MBA as a dual-functional linker to conjugate many aptamers and enhance the colloidal stability of nanotags. Compared with amide coupling method, this SA-biotin strategy confers the following advantages. First, the SA-biotin interaction is

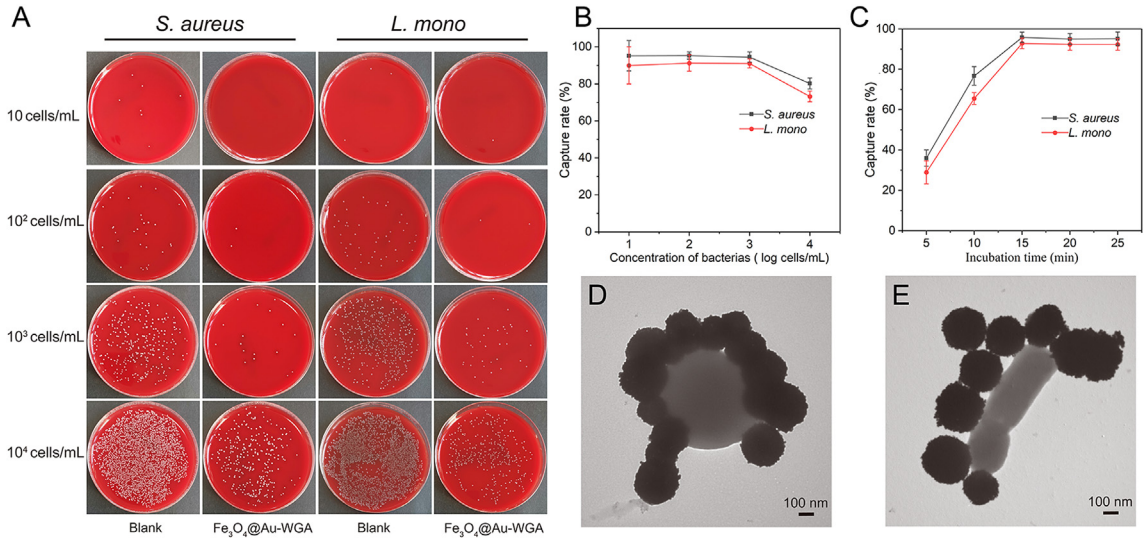

Fig. 2. Verification of the capture efficiency of Fe_3O_4@Au-WGA MNPs. (A) Photographs of the colonies on blood agar plates representing the amounts of remaining *S. aureus* and *L. mono* in the supernatant after Fe_3O_4@Au-WGA MNPs capture. Concentrations of *bacteria* ranged from 10 cells/mL to 10^4 cells/mL. (B) Corresponding capture efficiency of Fe_3O_4@Au-WGA MNPs for *S. aureus* and *L. mono*. (C) Capture efficiency of Fe_3O_4@Au-WGA MNPs versus incubation time. (D–E) TEM images of the formed Fe_3O_4@Au-WGA-*S. aureus* (D) and Fe_3O_4@Au-WGA-*L. mono* (E) complexes.

the rapid binding event with higher affinity than conventional antibody-antigen and aptamer-antigen interactions. Thus, the biotin–aptamer could be easily conjugated on the Au-SA in a short time. Second, SA has four domains for biotin-aptamer binding [44–46]. Hence, the amount of aptamer on SERS tags was increased by four times. Third, SA modification onto the AuNPs can ensure the high stability of nanotags in high-salt environment (Mg^{2+}) [47,48], which benefits the aptamers to open their secondary structure for bacteria binding.

The performance of conventional Au-aptamer tags and our proposed Au-SA/aptamer co-functionalized tags were compared by testing the same bacteria samples. As displayed in Fig. 3, the TEM images of Fe_3O_4@Au/bacteria/SERS tags complexes showed that the AuNP-SA/aptamer co-functionalized tags more effectively bind to *S. aureus* and *L. mono* (Fig. 3A and C) than common AuNP-aptamer tags (Fig. 3B and D). According to the increased number of AuNP-SA/aptamer tags onto the bacteria, the formed Fe_3O_4@Au/bacteria/SERS tags complexes generated higher DTNB and MBA signals than the AuNP-aptamer tags that formed sandwich complexes (Fig. 3E and F). In addition, the stability of AuNP-SA/aptamer SERS tags was better than that of AuNP-aptamer tags when the Mg^{2+} concentration in PBS solution was increased to 10 mM (Fig. S7). These results revealed the superior performance of AuNP-SA/aptamer co-functionalized tags for SERS-label based detection of bacteria.

Given that aptamers need time to open their secondary structure for target bacteria recognition, the reaction times of Au-SA/aptamer tags with *S. aureus* and *L. mono* should be optimized. As revealed in Fig. 4A, the number of SERS tags attached onto the surface of their target bacteria increased with the incubation time (15–45 min). No difference was observed in the TEM images of bacteria/SERS tags complexes when the reaction time of SERS tags and bacteria was increased from 45 min to 55 min. The SERS spectra of formed bacteria/SERS tags complexes were measured to support the TEM observation. As shown in Fig. 4B and C, the SERS intensity of *S. aureus*/tags and *L. mono*/tags complexes reached the maximum when the incubation time was 45 min. These results confirmed that the full binding of Au-SA/aptamer tags onto target bacteria can reach saturation within 45 min.

3.5. Detection of bacteria via the proposed SERS-label platform

To assess the detection sensitivity of the proposed method, *S. aureus* and *L. mono* with different concentrations (10^7-10 cells/mL) were spiked into PBS buffer to prepare standard bacteria samples. The accurate concentration of two bacteria in samples was determined by traditional plate counting as displayed in Fig. S8. The two groups bacterial samples were then tested via the proposed SERS-label platform under optimized conditions. Fig. 5A and C displays the SERS spectra of the formed Fe_3O_4@Au-WGA/bacteria/SERS tags sandwich complexes to *S. aureus* samples (10^7-0 cells/mL) and *L. mono* samples (10^7-0 cells/mL), respectively. The overall SERS signal from the tested samples gradually increased with the concentrations of *S. aureus*/*L. mono*. The typical Raman band at 1331 cm^{-1} of DTNB loaded SERS tags and 1588 cm^{-1} of MBA loaded SERS tags were chosen as the analytical signal to establish a linear relationship for *S. aureus* and *L. mono*, respectively. As shown in Fig. 5B and D, a strong linear relationship was found between the SERS signal at 1331 cm^{-1} and the logarithmic concentration of *S. aureus* and between SERS signal at 1588 cm^{-1} and the logarithmic concentration of *L. mono,* respectively, from 10^7 cells/mL to 10 cells/mL with correlation coefficient (R^2) = 0.993 for *S. aureus* and R^2 = 0.978 for *L. mono*. The LODs of the proposed platform for *S. aureus* and *L. mono* were 3 and 5 cells/mL, respectively, based on signal-to-noise ratio (SNR) of three criteria. Compared with the most of SERS label-based methods for bacteria detection, the proposed assay exhibited better performance including higher sensitivity, faster testing speed, and more detection channels (Table 1). These improvements in performance can be attributed to the superior capture capacity of WGA-modified Fe_3O_4@Au and the high binding efficiency of AuNP-SA/aptamer tags.

In actual food sample or biospecimen detection, the simultaneous screening of multiple bacterial pathogens in one sample is an urgent demand to effectively improve testing efficiency, reduce costs, and avoid misdiagnosis. Current mature methods (e.g., PCR, ELISA, and DNA sequence) for multiple bacteria sensitive and simultaneous screening are time consuming and labor intensive [7]. In theory, SERS-label immunoassays could easily achieve the sensitive detection of several targets in one test by using multiple

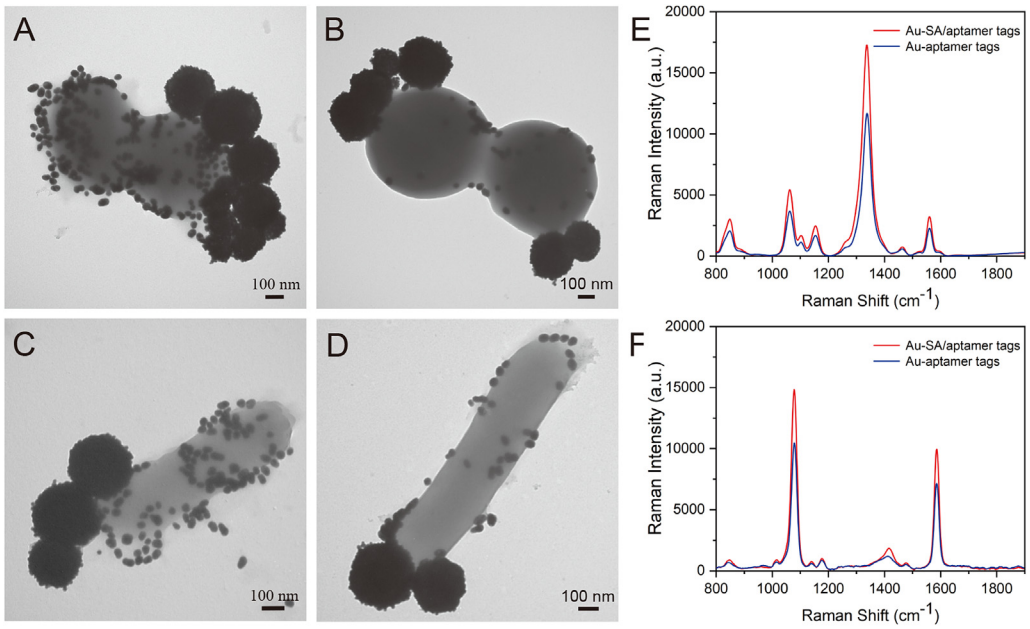

Fig. 3. Comparison of the binding ability of common AuNP-aptamer SERS tags and the proposed AuNP-SA/aptamer co-functionalized SERS tags. (A–D) TEM image of Fe_3O_4@Au-bacteria-SERS tags sandwich complexes: (A) Fe_3O_4@Au/*S. aureus*/AuNP-SA/aptamer, (B) Fe_3O_4@Au/*S. aureu*/AuNP-aptamer, (C) Fe_3O_4@Au/*L. momo*/AuNP-SA/aptamer, and (D) Fe_3O_4@Au/*L. momo*/AuNP-aptamer. (E–F) SERS intensity signal measured from Fe_3O_4@Au-WGA/bacteria complexes binding with AuNP-aptamer and AuNP-SA/aptamer co-functionalized SERS tags: (E) 10^5 cells/mL *S. aureus* and (F) 10^5 cells/mL *L. mono*.

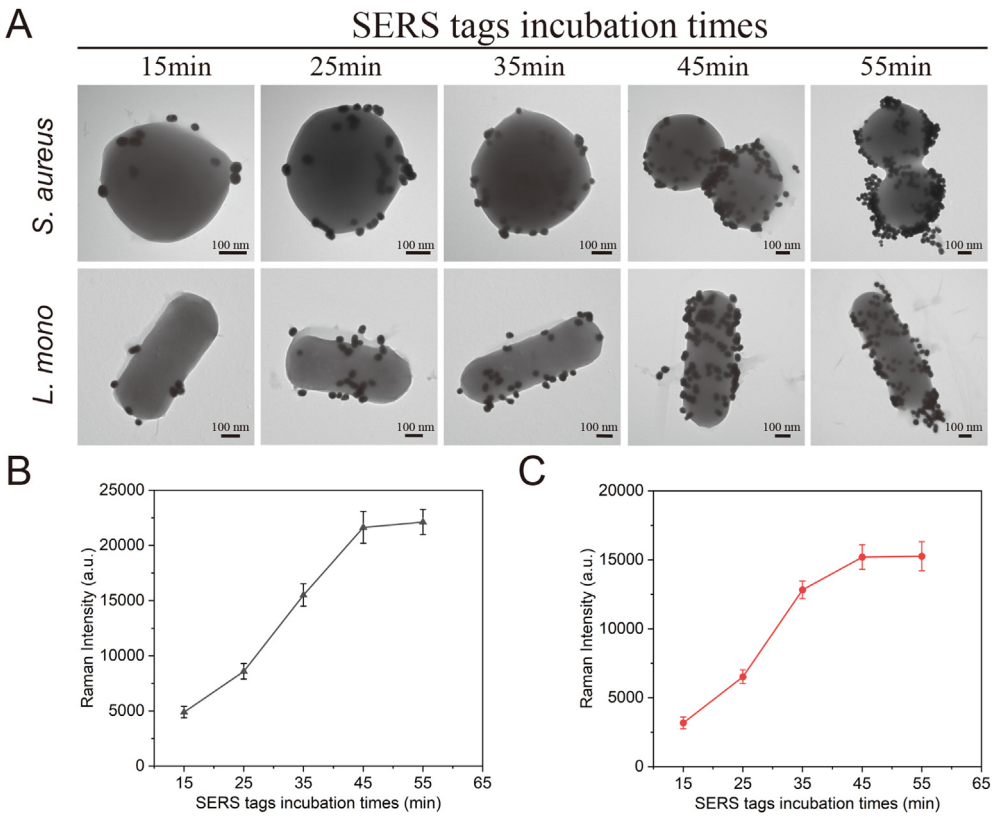

Fig. 4. (A) TEM images of obtained bacteria/tags complexes with different incubation times of AuNP-SA/aptamer tags. The SERS intensities at 1331 cm^{-1} for *S. aureus* (B) and 1588 cm^{-1} for *L. mono* (C) versus the incubation time of AuNP-SA/aptamer tags. Error bars represent the standard deviation of five repetitive experiments.

SERS tags with specific Raman molecules and recognition molecules. Therefore, the multiplex analysis ability of the proposed SERS-label platform was investigated by testing a mixture sample containing the same concentration of *S. aureus*/*L. mono*. As displayed in Fig. 6A, a mixed SERS spectrum of DTNB and MBA was observed for the mixture sample (red line), whereas the typical

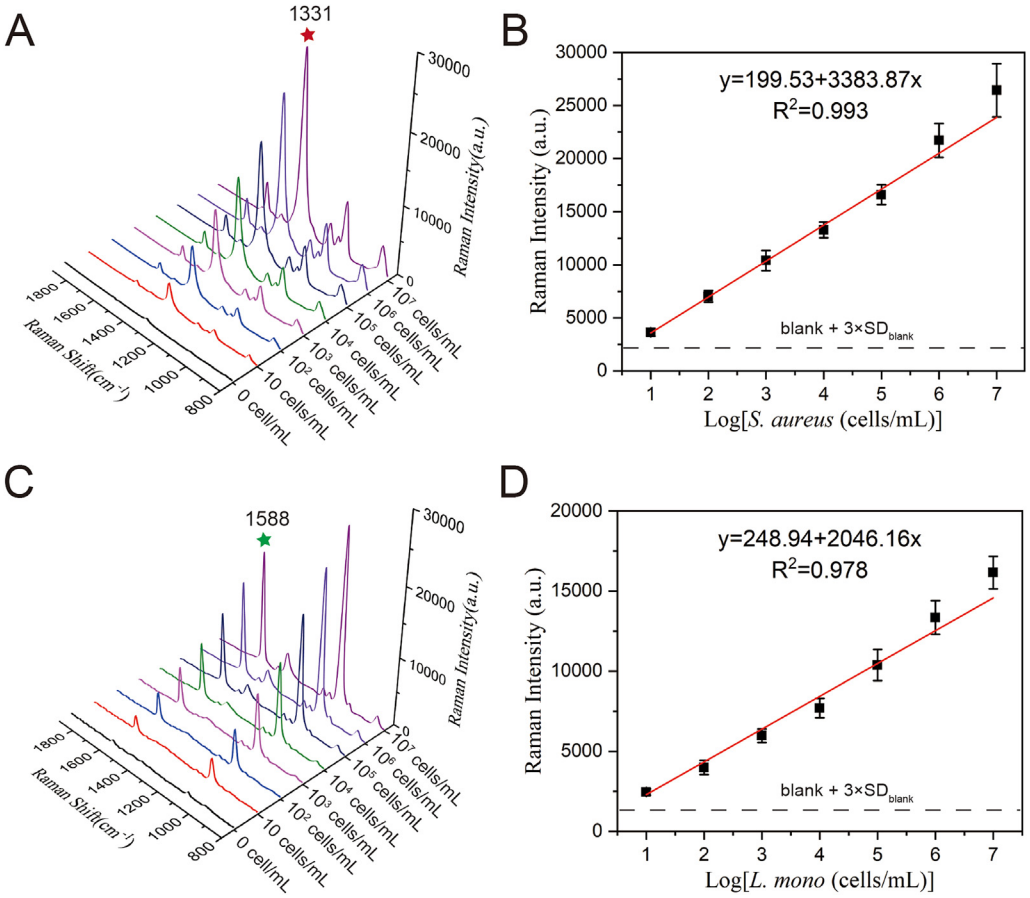

Fig. 5. SERS assay performance measured from the Fe_3O_4@Au-WGA/bacteria/SERS tags sandwich complexes with different concentrations (10^7–10 cells/mL) of (A) *S. aureus* and (C) *L. mono*. Corresponding calibration curves between the logarithms of pathogen concentrations and SERS intensities at 1331 cm^{-1} for *S. aureus* (B) and 1588 cm^{-1} for *L. mono* (D). Error bars represent the standard deviations from five independent assays.

Table 1
Comparison of other SERS label-based bacteria detection methods.

Biorecognition agents	Bacteria	LOD (cells/mL)	Assay time (min)	Reference
Two Aptamers	*S. aureus, S. typhi*	35, 15	170	Zhang. 2015 [49]
Two Antibodies	*S. aureus*	10	120	Wang. 2016 [50]
Vancomycin/aptamer	*S. aureus, E. coli*	20, 50	90	Zhang. 2018 [19]
Peptide/PMBA	*E. coli, S. aureus* *P. aeruginosa*	10	>120	Kaisong. 2018 [51]
Two Aptamers	*E. coli, S. aureus*	10^2	>90	Diaz. 2019 [52]
Antibody	*S. typhi*	100	180	Chattopadhyay et al., 2019 [53]
PMBA/vancomycin	*S. aureus*	10	>90	Gao et al., 2020 [54]
WGA/SA-aptamer	*S. aureus, L. mono*	3, 5	90	This work

Abbreviations: PMBA: 4-mercaptophenylboronic acid.

SERS spectra of DTNB (blue line) or MBA (green line) were only detected in the presence of *S. aureus* or *L. mono*, respectively. On the basis of these SERS signals, the major Raman band at 1331 cm^{-1} of DTNB modified-tags, and the second major band at 1588 cm^{-1} of MBA modified-tags can be differentiated without overlapping each other and thus could be served as the distinct signatures for *S. aureus* and *L. mono* identification, respectively.

The multiplexing capability and selectivity of the proposed method were further examined by testing different bacterial samples containing other common pathogenic bacteria including *S. epidermidis*, *P. aeruginosa*, *E. coli*, *A. baumannii*, *S. sonnei*, and *S. typhi* as the interference bacterium. The Fe_3O_4@Au-WGA MNPs were separately added into 1 mL of target bacteria samples (10^3 cells/mL) and non-target bacteria samples (10^7 cells/mL) using the developed protocol. The formed Fe_3O_4@Au-bacteria complexes were magnetically collected and incubated with two kinds of SERS tags for *S. aureus* and *L. mono*. The SERS signals measured from each sample in Fig. 6B showed no SERS intensity at 1331 and 1588 cm^{-1} for all non-target bacteria. The positive groups for *S. aureus*, *L. mono*, and *S. aureus*/*L. mono* mixture exhibited distinct SERS intensity at 1331, 1588 cm^{-1}, and 1331/1588 cm^{-1}, respectively. In addition, the reproducibility of our method was evaluated by testing 10 *S. aureus* and *L. mono* samples (10^5 cells/mL). As revealed in Fig. 6C and D, relatively uniform SERS spectra of DTNB and MBA were observed for *S. aureus* and *L. mono* groups, and their relative standard deviation (RSD) values were lower than 7.03%. These results confirmed

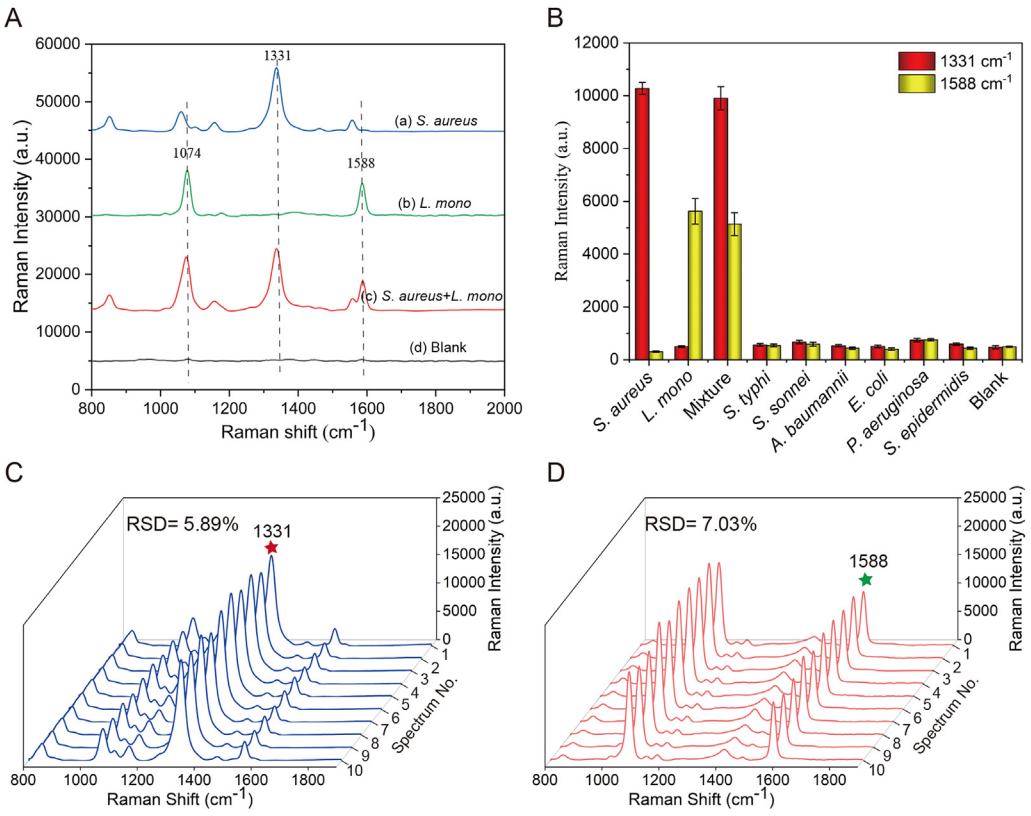

Fig. 6. (A) Multiple detection of *S. aureus* and *L. mono* in one sample based on our proposed dual-recognition SERS platform. (B) Raman intensities for *S. aureus*, *L. mono* and six interfering bacteria. The tested concentration of target bacteria was 10^3 cells/mL, whereas the concentration of interfering bacteria groups was maintained at 10^7 cells/mL. (C–D) Repeatability of SERS assay for 10^5 cells/mL of target bacteria: (C) *S. aureus* and (D) *L. mono*. Each spectrum was obtained from the average SERS intensities of 20 random measurements.

that the proposed SERS platform possesses good specificity and reproducibility for targeted bacteria detection.

3.6. Real sample analysis

The applicability of this platform in actual samples was verified by comparing the capture efficiency of *S. aureus* and *L. mono* in three kinds of real samples including orange juice, extracts of lettuce, and human urine. As shown in Fig. S9, the capture efficiency of the proposed magnetic separation system was not affected when applied in all the tested real samples. All samples were spiked with *S. aureus* and *L. mono* at different concentration levels (50, 500, and 5000 cells/mL) to further test the performance of the SERS dual recognition strategy in practical applications. As shown in Table 2, the recovery rates for *S. aureus* and *L. mono* ranged from 88% to 110% and 86%–111%, respectively, indicating the applicability and good accuracy of the proposed method for the quantification of *S. aureus* and *L. mono* in real samples. The low RSD (4.2–10%) of repeated measurement experiments exhibited the good repeatability of the SERS assay. In consideration of the good capture ability of Fe_3O_4@Au-WGA to other bacteria including *S. epidermidis*, *P. aeruginosa*, and *E. coli*, the proposed SERS platform can be easily expanded to detect these pathogens by using specific aptamers. Thus, this method has potential as a universal tool for the sensitive detection of multiple bacteria.

4. Conclusion

An ultra-sensitive and selective SERS platform was developed by using WGA-modified Fe_3O_4@Au MNPs to rapidly capture bacteria from samples and SA/aptamer co-functionalized SERS tags to provide strong and stable SERS signals. The Fe_3O_4@Au-WGA MNPs

Table 2
Recovery efficiency of *S. aureus and L. mono* detected in real samples. using the proposed SERS-based platform.

Samples	Spiked (cells/mL)	Measured (cells/mL)	Recovery (%)	RSD (%)
Orange juice	50/50	55/46	110.0/92.0	5.1/7.7
	500/500	543/527	108.6/105.4	7.1/6.3
	5000/5000	4677/4878	93.5/97.6	6.8/4.8
Extracts of lettuce	50/50	47/43	94.0/86	5.1/4.0
	500/500	497/512	99.4/102.4	5.4/7.3
	5000/5000	5305/4749	106.1/95.0	7.7/10.0
Human urine	50/50	44/54	88.0/108.0	4.4/9.2
	500/500	466/451	93.2/90.2	5.0/5.7
	5000/5000	5407/5551	108.1/111.0	4.2/7.8

Note. The value before and after "/" represent the corresponding items of *S. aureus* and *L.* mono, respectively.

showed excellent binding ability to at least eight bacterial species including *S. epidermidis*, *P. aeruginosa*, *S. aureus*, *L. mono*, *E. coli*, *A. baumannii*, *S. sonnei*, and *S. typhi* and can achieve a high capture efficiency for *S. aureus* (94.39%) and *L. mono* (90.79%) within 15 min. The SA/aptamer co-functionalized AuNPs exhibited superior affinity to target bacteria and better stability in high salt solution compared with the commonly used aptamer-modified SERS tags. With its dual-recognition pattern, the proposed SERS platform can simultaneously detect *S. aureus* and *L. mono* by measuring the SERS intensities of DTNB at 1331 cm^{-1} and MBA at 1588 cm^{-1}. Good linear responses with the two bacteria were observed in the ranges of 10–10^7 cells/mL. The LODs of the assay for *S. aureus* and *L. mono* were 3 and 5 cells/mL, respectively. The potential application of this platform was also evaluated using several kinds of real food samples (juice, extracts of lettuce), and human urine. This work is the first to use WGA and aptamer based dual-recognition biosensor to simultaneously detect *S. aureus* and *L. mono* by SERS-label assay. By changing the specific aptamers, the proposed method has strong potential as a sensitive and universal detection tool for the multiplex detection of other pathogens.

Declaration of competing interest

The authors declare that they have no known competing financial interests or personal relationships that could have appeared to influence the work reported in this paper.

Acknowledgements

This research was supported by the National Natural Science Foundation of China (81871734, 81471994), the Natural Science Foundation of Anhui Province (Grant no. 1908085QB85), the National S&T Major Project for Infectious Diseases Control (Grant nos. 2018ZX10712001-010, 2018ZX10101003-001), and the Postgraduate Research & Practice Innovation Program of Jiangsu Province (No. KYCX20_2472). The authors Siyun Cheng and Zhijie Tu contributed equally to this work.

Appendix A. Supplementary data

Supplementary data to this article can be found online at https://doi.org/10.1016/j.aca.2021.339155.

References

[1] W.I. Lee, Y. Park, S. Shrivastava, T. Jung, M. Meeseepong, J. Lee, et al., A fully integrated bacterial pathogen detection system based on count-on-a-cartridge platform for rapid, ultrasensitive, highly accurate and culture-free assay, Biosens. Bioelectron. 152 (2020) 112007.
[2] J. Dietvorst, L. Vilaplana, N. Uria, M.-P. Marco, X. Muñoz-Berbel, Current and near-future technologies for antibiotic susceptibility testing and resistant bacteria detection, rAC-Trend Anal Chem. 127 (2020) 115891.
[3] D.D. Galvan, Q. Yu, Surface-enhanced Raman scattering for rapid detection and characterization of antibiotic-resistant bacteria, Adv Healthc Mater 7 (2018), e1701335.
[4] T. Charalampous, G.L. Kay, H. Richardson, A. Aydin, R. Baldan, C. Jeanes, et al., Nanopore metagenomics enables rapid clinical diagnosis of bacterial lower respiratory infection, Nat. Biotechnol. 37 (2019) 783–792.
[5] Y. Zhang, Y. Tang, C. Tan, W. Xu, Toward nanopore electrospray mass spectrometry: nanopore effects in the analysis of bacteria, ACS Cent. Sci. 6 (2020) 1001–1008.
[6] M. Boolchandani, A.W. D'Souza, G. Dantas, Sequencing-based methods and resources to study antimicrobial resistance, Nat. Rev. Genet. 20 (2019) 356–370.
[7] K. Zhang, H. Li, W. Wang, J. Cao, N. Gan, H. Han, Application of multiplexed aptasensors in food contaminants detection, ACS Sens. 5 (2020) 3721–3738.
[8] E. Cesewski, B.N. Johnson, Electrochemical biosensors for pathogen detection, Biosens. Bioelectron. 159 (2020) 112214.
[9] S. Kaushik, U.K. Tiwari, S.S. Pal, R.K. Sinha, Rapid detection of Escherichia coli using fiber optic surface plasmon resonance immunosensor based on biofunctionalized Molybdenum disulfide (MoS2) nanosheets, Biosens. Bioelectron. 126 (2019) 501–509.
[10] W. Wu, C. Yu, Q. Wang, F. Zhao, H. He, C. Liu, et al., Research advances of DNA aptasensors for foodborne pathogen detection, Crit. Rev. Food Sci. Nutr. 60 (2020) 2353–2368.
[11] J. Langer, D. Jimenez de Aberasturi, J. Aizpurua, R.A. Alvarez-Puebla, B. Auguié, J.J. Baumberg, et al., Present and future of surface-enhanced Raman scattering, ACS Nano 14 (2020) 28–117.
[12] W. Shen, C. Wang, X. Yang, C. Wang, Z. Zhou, X. Liu, et al., Synthesis of raspberry-like nanogapped Fe3O4@Au nanocomposites for SERS-based lateral flow detection of multiple tumor biomarkers, J. Mater. Chem. C. 8 (2020) 12854–12864.
[13] C. Wang, C. Wang, X. Wang, K. Wang, Y. Zhu, Z. Rong, et al., Magnetic SERS strip for sensitive and simultaneous detection of respiratory viruses, ACS Appl. Mater. Interfaces 11 (2019) 19495–19505.
[14] H. Liu, E. Dai, R. Xiao, Z. Zhou, M. Zhang, Z. Bai, et al., Development of a SERS-based lateral flow immunoassay for rapid and ultra-sensitive detection of anti-SARS-CoV-2 IgM/IgG in clinical samples, Sensor. Actuator. B Chem. 329 (2021) 129196.
[15] C.Y. Wen, Y.Z. Jiang, X.Y. Li, M. Tang, L.L. Wu, J. Hu, et al., Efficient enrichment and analyses of bacteria at ultralow concentration with quick-response magnetic nanospheres, ACS Appl. Mater. Interfaces 9 (2017) 9416–9425.
[16] Z. Zhou, R. Xiao, S. Cheng, S. Wang, L. Shi, C. Wang, et al., A universal SERS-label immunoassay for pathogen bacteria detection based on Fe3O4@Au-aptamer separation and antibody-protein A orientation recognition, Anal. Chim. Acta 1160 (2021) 338421.
[17] Y. Pang, J. Shi, X. Yang, C. Wang, Z. Sun, R. Xiao, Personalized detection of circling exosomal PD-L1 based on Fe3O4@TiO2 isolation and SERS immunoassay, Biosens. Bioelectron. 148 (2020) 111800.
[18] Y. Li, C. Lu, S. Zhou, M.-L. Fauconnier, F. Gao, B. Fan, et al., Sensitive and simultaneous detection of different pathogens by surface-enhanced Raman scattering based on aptamer and Raman reporter co-mediated gold tags, Sensor. Actuator. B Chem. 317 (2020) 128182.
[19] C. Zhang, C. Wang, R. Xiao, L. Tang, J. Huang, D. Wu, et al., Sensitive and specific detection of clinical bacteria via vancomycin-modified Fe3O4@Au nanoparticles and aptamer-functionalized SERS tags, J. Mater. Chem. B 6 (2018) 3751–3761.
[20] J. Chen, S.M. Andler, J.M. Goddard, S.R. Nugen, V.M. Rotello, Integrating recognition elements with nanomaterials for bacteria sensing, Chem. Soc. Rev. 46 (2017) 1272–1283.
[21] Y. Liu, H. Zhou, Z. Hu, G. Yu, D. Yang, J. Zhao, Label and label-free based surface-enhanced Raman scattering for pathogen bacteria detection: a review, Biosens. Bioelectron. 94 (2017) 131–140.
[22] D. Cheng, M. Yu, F. Fu, W. Han, G. Li, J. Xie, et al., Dual recognition strategy for specific and sensitive detection of bacteria using aptamer-coated magnetic beads and antibiotic-capped gold nanoclusters, Anal. Chem. 88 (2016) 820–825.
[23] Z. Huang, J. Peng, J. Han, G. Zhang, Y. Huang, M. Duan, et al., A novel method based on fluorescent magnetic nanobeads for rapid detection of Escherichia coli O157:H7, Food Chem. 276 (2019) 333–341.
[24] X. Liu, X. Yang, K. Li, H. Liu, R. Xiao, W. Wang, et al., Fe3O4@Au SERS tags-based lateral flow assay for simultaneous detection of serum amyloid A and C-reactive protein in unprocessed blood sample, Sensor. Actuator. B Chem. 320 (2020) 128350.
[25] F. Charbgoo, M. Ramezani, M. Darroudi, Bio-sensing applications of cerium oxide nanoparticles: advantages and disadvantages, Biosens. Bioelectron. 96 (2017) 33–43.
[26] R. Gupta, A. Kumar, S. Kumar, A.K. Pinnaka, N.K. Singhal, Naked eye colorimetric detection of Escherichia coli using aptamer conjugated graphene oxide enclosed Gold nanoparticles, Sensor. Actuator. B Chem. 329 (2021) 129100.
[27] K. Wang, S. Li, M. Petersen, S. Wang, X. Lu, Detection and characterization of antibiotic-resistant bacteria using surface-enhanced Raman spectroscopy, Nanomaterials (2018) 8.
[28] D. Neumann, C.M. Lehr, H.P. Lenhof, O. Kohlbacher, Computational modeling of the sugar-lectin interaction, Adv. Drug Deliv. Rev. 56 (2004) 437–457.
[29] Y. Wang, Z. Ye, C. Si, Y. Ying, Monitoring of Escherichia coli O157:H7 in food samples using lectin based surface plasmon resonance biosensor, Food Chem. 136 (2013) 1303–1308.
[30] F. Mi, M. Guan, C. Hu, F. Peng, S. Sun, X. Wang, Application of lectin-based biosensor technology in the detection of foodborne pathogenic bacteria: a review, Analyst 146 (2021) 429–443.
[31] X.M. Guotai Yanga, Yutong Wanga, Mingyao Yana, Zoraida P. Aguilarb, Hengyi Xua, 2-Step lectin-magnetic separation (LMS) strategy combined with AuNPsbased colorimetric system for S. aureus detection in blood, Sensor. Actuator. B Chem. 279 (2019) 87–94.
[32] Z. Li, Y. Fu, W. Fang, Y. Li, Electrochemical impedance immunosensor based on self-assembled monolayers for rapid detection of Escherichia coli O157:H7 with signal amplification using lectin, Sensors 15 (2015) 19212–19224.
[33] M. Masigol, N. Fattahi, N. Barua, B.S. Lokitz, S.T. Retterer, T.G. Platt, et al., Identification of critical surface parameters driving lectin-mediated capture of bacteria from solution, Biomacromolecules 20 (2019) 2852–2863.
[34] M.V. Mikaelyan, G.G. Poghosyan, O.D. Hendrickson, B.B. Dzantiev, V.K. Gasparyan, Wheat germ agglutinin and Lens culinaris agglutinin sensitized anisotropic silver nanoparticles in detection of bacteria: a simple photometric assay, Anal. Chim. Acta 981 (2017) 80–85.
[35] N. Batool, S. Yoon, S. Imdad, M. Kong, H. Kim, S. Ryu, et al., An antibacterial

nanorobotic approach for the specific targeting and removal of multiple drug-resistant Staphylococcus aureus, Small (2021), e2100257.
[36] L. Radoshevich, P. Cossart, Listeria monocytogenes: towards a complete picture of its physiology and pathogenesis, Nat. Rev. Microbiol. 16 (2018) 32–46.
[37] C. Wang, W. Shen, Z. Rong, X. Liu, B. Gu, R. Xiao, et al., Layer-by-layer assembly of magnetic-core dual quantum dot-shell nanocomposites for fluorescence lateral flow detection of bacteria, Nanoscale 12 (2020) 795–807.
[38] X. Liu, X. Yang, K. Li, H. Liu, R. Xiao, W. Wang, et al., Fe3O4@Au SERS tags-based lateral flow assay for simultaneous detection of serum amyloid A and C-reactive protein in unprocessed blood sample, Sensor. Actuator. B Chem. 320 (2020) 128350.
[39] C. Wang, J. Wang, M. Li, X. Qu, K. Zhang, Z. Rong, et al., A rapid SERS method for label-free bacteria detection using polyethylenimine-modified Au-coated magnetic microspheres and Au@Ag nanoparticles, Analyst 141 (2016) 6226–6238.
[40] C. Wang, X. Yang, B. Gu, H. Liu, Z. Zhou, L. Shi, et al., Sensitive and simultaneous detection of SARS-CoV-2-specific IgM/IgG using lateral flow immunoassay based on dual-mode quantum dot nanobeads, Anal. Chem. 92 (2020) 15542–15549.
[41] J. Wang, X. Wu, C. Wang, N. Shao, P. Dong, R. Xiao, et al., Magnetically assisted surface-enhanced Raman spectroscopy for the detection of Staphylococcus aureus based on aptamer recognition, ACS Appl. Mater. Interfaces 7 (2015) 20919–20929.
[42] Z. Cheng, N. Choi, R. Wang, S. Lee, K.C. Moon, S.Y. Yoon, et al., Simultaneous detection of dual prostate specific antigens using surface-enhanced Raman scattering-based immunoassay for accurate diagnosis of prostate cancer, ACS Nano 11 (2017) 4926–4933.
[43] W. Zhang, S. Tang, Y. Jin, C. Yang, L. He, J. Wang, et al., Multiplex SERS-based lateral flow immunosensor for the detection of major mycotoxins in maize utilizing dual Raman labels and triple test lines, J. Hazard Mater. 393 (2020) 122348.
[44] C.N. Loynachan, M.R. Thomas, E.R. Gray, D.A. Richards, J. Kim, B.S. Miller, et al., Platinum nanocatalyst amplification: redefining the gold standard for lateral flow immunoassays with ultrabroad dynamic range, ACS Nano 12 (2018) 279–288.
[45] L. Bi, X. Wang, X. Cao, L. Liu, C. Bai, Q. Zheng, et al., SERS-active Au@Ag core-shell nanorod (Au@AgNR) tags for ultrasensitive bacteria detection and antibiotic-susceptibility testing, Talanta 220 (2020) 121397.
[46] J. Ko, C. Lee, J. Choo, Highly sensitive SERS-based immunoassay of aflatoxin B1 using silica-encapsulated hollow gold nanoparticles, J. Hazard Mater. 285 (2015) 11–17.
[47] X. Fu, J. Wen, J. Li, H. Lin, Y. Liu, X. Zhuang, et al., Highly sensitive detection of prostate cancer specific PCA3 mimic DNA using SERS-based competitive lateral flow assay, Nanoscale 11 (2019) 15530–15536.
[48] G. Lai, J. Wu, H. Ju, F. Yan, Streptavidin-functionalized silver-nanoparticle-enriched carbon nanotube tag for ultrasensitive multiplexed detection of tumor markers, Adv. Funct. Mater. 21 (2011) 2938–2943.
[49] H. Zhang, X. Ma, Y. Liu, N. Duan, S. Wu, Z. Wang, et al., Gold nanoparticles enhanced SERS aptasensor for the simultaneous detection of Salmonella typhimurium and Staphylococcus aureus, Biosens. Bioelectron. 74 (2015) 872–877.
[50] J. Wang, X. Wu, C. Wang, Z. Rong, H. Ding, H. Li, et al., Facile synthesis of Au-coated magnetic nanoparticles and their application in bacteria detection via a SERS method, ACS Appl. Mater. Interfaces 8 (2016) 19958–19967.
[51] a.Q.M. Kaisong Yuan, ‡b Xinjie Guo, a Youwei Xu, d Danting Yang, e Beatriz Jurado Sánchez, a.C.L. c Bingbing Sheng, a a Ziwei Hu, f.H.M. Guangchao Yu, f Hao Gao, *a Christoph Haisch, g Reinhard Niessner, g Zhengjing Jiang*a, Haibo Zhou, Antimicrobial peptide based magnetic recognition elements and Au@Ag-GO SERS tags with stable internal standards: a three in one biosensor for isolation, discrimination and killing of multiple bacteria in whole blood, Chem. Sci. 9 (2018) 8781–8795.
[52] S. Diaz-Amaya, L.K. Lin, A.J. Deering, L.A. Stanciu, Aptamer-based SERS biosensor for whole cell analytical detection of E. coli O157:H7, Anal. Chim. Acta 1081 (2019) 146–156.
[53] S. Chattopadhyay, P.K. Sabharwal, S. Jain, A. Kaur, H. Singh, Functionalized polymeric magnetic nanoparticle assisted SERS immunosensor for the sensitive detection of S. typhimurium, Anal. Chim. Acta 1067 (2019) 98–106.
[54] X. Gao, Y. Yin, H. Wu, Z. Hao, J. Li, S. Wang, et al., Integrated SERS platform for reliable detection and photothermal elimination of bacteria in whole blood samples, Anal. Chem. 93 (2020) 1569–1577.